
Stress characterization of autofrettaged thick-walled cylinders

J. M. Kihiu, S. M. Mutuli and G. O. Rading

Department of Mechanical Engineering, University of Nairobi, PO Box 30197, Nairobi, Kenya

Abstract The inaccessibility of commercial software has necessitated the development of low-cost, general-purpose finite element method (FEM) computer programs for structural analysis. Using the FEM program, the elastic, elastic-plastic, residual and service stresses and displacements in a closed ended, thick-walled cylinder under internal pressure were established. The displacement formulation was implemented and eight-noded brick isoparametric elements chosen. The frontal solution technique and the incremental theory of plasticity were used, as only limited computing facilities were available. The results were found to be in very good agreement with the through-thickness analytical values. The benefits of autofrettage were demonstrated and an optimum overstrain of 16% established for a cylinder with a thickness ratio of 2. The material economy achieved through autofrettage and the limitations imposed are illustrated. The FEM program could therefore be reliably used for other complex geometries and load conditions.

Keywords elastic; plastic; overstrain; incremental; economy

Notation

FEM	finite element method
G	modulus of rigidity
H'	tangent modulus
I_1	first stress invariant
Y_s	yield stress
$\bar{\epsilon}^n$	effective strain
$\bar{\sigma}$	effective stress
σ_i	principal stress components
τ_{ij}	shear stress components

Introduction

Pressure vessels are now widely used in nuclear power plants for steam and power generation [1]. Other pressure vessel applications may involve pressures as high as 1380 MPa and temperatures of up to 300°C, resulting in the pressure vessel material holding immense potential energy exerted by the working fluid [2]. The process fluid may also be a source of hydrogen embrittlement and/or stress corrosion cracking [3]. Such high-pressure vessels require proper understanding of the stress levels and their distributions in order to have fail-safe designs or even to minimize the probability of disruptive failures. Past pressure vessel catastrophic failures, arising from lack of understanding of stress levels, material properties and fluid/structure environmental interactions, particularly early in the last century [4–6], were very expensive in terms of losses in materials and human life, and they were the main

impetus for the early studies of stresses in cylinders of various materials [7]. Later on, the stress distribution in critical sections and metallurgical failure aspects were given more emphasis.

High-pressure vessels are now of great importance in many industries [1] and their economic use often depends upon the occurrence of small, controlled, permanent deformations. Before commissioning, pressure vessels are normally pressure tested at an overstrain pressure of 1.25–1.5 times the design pressure [8,9] in order to test for leakages. This process results in yielding of the bore and may also advantageously lead to catastrophic failure for poorly designed or fabricated vessels. Vessels with brittle characteristics may also fail at this stage. After overstraining, residual stresses are left in the cylinder and the nature of these residual stresses is now widely known. However, the residual stress levels are not documented for use in service or during de-rating after periodic inspections. In service, the vessels are able to carry a much higher load before re-yielding than would be the case without the leak test. Overstraining beyond the leak test pressure is usually carried out during manufacture [10] and this technique is called autofrettage or self-hooping.

The first aim of this work is to develop a finite element method (FEM) computer program to determine the elastic, elastic-plastic, residual and service stresses in a thick-walled cylinder for various overstrains and compare them with analytical results. It is useful to note that commercial FEM packages are not readily available to the authors of this work due to the high costs involved, and locally developed programs are the only solution for serious research. The second aim is to determine an optimum level of overstrain and to quantify the advantages of autofrettage.

Literature review

Elastic-plastic stresses

The need to reduce pressure vessel material costs led to various studies on the bursting strength of cylinders as a basis of design [11–14] and various formulae were proposed [15,16]. This was due to the realization that elastic service designs did not fully utilize the pressure-carrying potential of the pressure vessel materials. High pressures and temperatures required high-strength thick sections, which were later found to be weak in resisting crack propagation, while thinner sections had better fracture toughness properties [10]. Advances in technology and the interest in the limit state design therefore made the inclusion of non-linear effects such as the elastic-plastic behaviour desirable in the analysis and design of many structures. To subject the pressure vessel to elastic-plastic stress conditions it was necessary first to establish the relevant constitutive stress–strain laws [17–20].

A stiffness method for elastic-plastic problems which enabled the equilibrium equations to be expressed in terms of displacements was developed [21]. The use of stiffness coefficients removed the need to trace the expansion of the elastic-plastic boundary during the actual solution of the governing differential equations. The change of slope of the stress–strain diagram at yield and the non-linearity of the problem were found to prevent elastic-plastic problems from being solved by a

closed form analysis. A technique was proposed for dealing with this problem, based on an estimate of the strains that would be caused by the next increment of load. The method was found to work for closed ended tubes under internal pressure, though it was not suitable for the analysis of perfectly plastic materials or materials with very small strain hardening exponents.

The plastic stress–strain matrix derivable by inverting the Pradtl–Reuss equations in the plasticity theory was proposed in the solution of continuum elastic–plastic problems using the FEM [22]. The method uses the small and varying increments of load just sufficient to cause yield in the successive elements and the following plastic stress–strain constitutive equation was developed:

$$[D^p] = \frac{2G}{\frac{2^{-2}}{3} \sigma \left(1 + \frac{H'}{3G}\right)} [Z] \quad (1)$$

where,

$$[Z] = \begin{bmatrix} \sigma_{Dx}^2 & \sigma_{Dx}\sigma_{Dy} & \sigma_{Dx}\sigma_{Dz} & \sigma_{Dx}\tau_{xy} & \sigma_{Dx}\tau_{yz} & \sigma_{Dx}\tau_{xz} \\ \sigma_{Dx}\sigma_{Dy} & \sigma_{Dy}^2 & \sigma_{Dy}\sigma_{Dz} & \sigma_{Dy}\tau_{xy} & \sigma_{Dy}\tau_{yz} & \sigma_{Dy}\tau_{xz} \\ \sigma_{Dx}\sigma_{Dz} & \sigma_{Dy}\sigma_{Dz} & \sigma_{Dz}^2 & \sigma_{Dz}\tau_{xy} & \sigma_{Dz}\tau_{yz} & \sigma_{Dz}\tau_{xz} \\ \sigma_{Dx}\tau_{xy} & \sigma_{Dy}\tau_{xy} & \sigma_{Dz}\tau_{xy} & \tau_{xy}^2 & \tau_{xy}\tau_{yz} & \tau_{xy}\tau_{xz} \\ \sigma_{Dx}\tau_{yz} & \sigma_{Dy}\tau_{yz} & \sigma_{Dz}\tau_{yz} & \tau_{xy}\tau_{yz} & \tau_{yz}^2 & \tau_{yz}\tau_{xz} \\ \sigma_{Dx}\tau_{xz} & \sigma_{Dy}\tau_{xz} & \sigma_{Dz}\tau_{xz} & \tau_{xy}\tau_{xz} & \tau_{yz}\tau_{xz} & \tau_{xz}^2 \end{bmatrix} \quad (2)$$

$$\bar{\sigma} = \frac{1}{\sqrt{2}} \left[(\sigma_1 - \sigma_2)^2 + (\sigma_2 - \sigma_3)^2 + (\sigma_3 - \sigma_1)^2 \right]^{\frac{1}{2}} \quad (3)$$

$$\{\sigma_D\} = \{\sigma_x - I_1/3, \sigma_y - I_1/3, \sigma_z - I_1/3, \tau_{xy}, \tau_{yz}, \tau_{xz}\} \quad (4)$$

The effect of the yield stress and the strain hardening exponent of the material on the stress and strain levels was studied in a bore expanding test using the incremental theory of plasticity [23]. By considering that the effective stress is given by the equation:

$$\bar{\sigma} = Y_s + C\bar{\epsilon}^n \quad (5)$$

and that:

$$\bar{\sigma} \approx C\bar{\epsilon}^n \quad (6)$$

where $\bar{\sigma}$ is the effective stress, $\bar{\epsilon}$ is the effective strain, C is a material constant and n is a strain hardening exponent, the indeterminacy of the initial conditions were eliminated by the use of the above approximation.

Finite size deformations, as found in elastic–plastic metal forming problems, have been found to introduce numerical instability in FEM analysis. However, this has been overcome by modifying the stiffness formulation by means of the mean normal technique [24]. A FEM variational technique that allows considerably larger loading steps in the load increment method of elastic–plastic analysis without deviating from

its non-linear load–deformation relationship has been developed [25]. The method was found to result in a 240% improvement in computational efficiency and a substantial reduction in the number of load steps. The applicability of the isoparametric elements and the order of computation times involved have also been studied for three-dimensional FEM elastic-plastic problems [26]. The conventional FEM has been found to be weak in predicting surface stresses, where phenomena of interest usually occur. However, improved results have been obtained by careful modification of the surface element shape functions [27–29]. Current FEM practitioners use commercial software and may not have the intricate, detailed knowledge of the FEM, particularly in elastic-plastic analysis.

Residual stresses

The determination of residual stresses is important in fracture analysis and fatigue life estimation and in the assessment of shakedown in elastic-plastic structures. Various solutions in considerable disagreement have been obtained by considering different mathematical methods, end conditions and material models. Different assumptions for the material properties, such as compressibility, yield criteria, flow rule, hardening rule and Bauschinger effect [30], have also produced differing results.

The theory of autofrettage and the distribution of residual stresses in strain hardening materials for open cylinders have been well described [31] and the von Mises theory has been found to be more realistic in accounting for end conditions. The optimum overstrain has been defined as the maximum overstrain that does not result in reverse yielding and that is associated with the greatest amount of elastic stress release. Another definition of the optimum overstrain is that which minimizes the maximum effective service stress for a given service pressure [32]. For a cylinder with a thickness ratio of 2 and a service pressure of 200 MPa, the optimum overstrain was found to be 20%. For a service pressure of 500 MPa, the optimum overstrain was found to be 40%. An optimum overstrain radius equal to the geometric mean radius, $(R_i R_o)^{0.5}$, has been proposed for medium-strength steels. For high-strength steels, the optimum overstrain is slightly less [33]. A definition of the optimum overstrain based on the material economy and considering reverse yielding would be more appropriate.

A material removal method for measuring the level of overstrain in a thick-walled cylinder involving the axisymmetric release of the stresses by introducing radial cuts in the cylinder has been proposed [34,35]. The experimental method yielded a simple empirical relation which enabled determination of the overstrain from measurements of released strain. A method of estimating residual stresses by use of two FEM analyses has been proposed, but is applicable only to local regions of interest, such as notches [36]. The hole-drilling destructive procedure has been widely used for evaluating residual stresses [37]. Other material-removal methods coupled with FEM reconstruction procedures have been developed [38]. For plain cylinders, it has been established that the residual stress distributions may be obtained by thermal load simulation [39]. The selection of service pressures after autofrettage has not been well addressed, though it is very important.

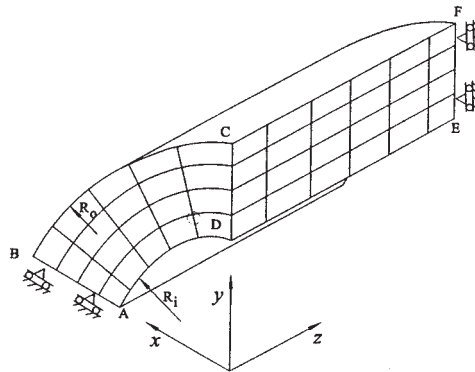


Fig. 1 *Discretization of plain cylinder.*

Methodology

A FEM computer program in FORTRAN code, having elastic and elastic-plastic capabilities, was developed to carry out the pre-processing, processing and post-processing procedures. The pressure vessel material was a high-strength SA-372 steel, which has a yield stress of 450 N/mm^2 , a Poisson's ratio of 0.29 and a Young's modulus of $209 \times 10^3 \text{ N/mm}^2$ [40]. Due to symmetry, the cylinder was modelled and discretized as shown in Fig. 1. The geometrical inputs for complete description of the geometry were the inner radius (75 mm), outer radius (150 mm), length of cylinder (9 times the cylinder thickness), geometrical ratio of nodal spacing in the radial direction (1.15), number of elements along arc AD (20), number of elements in the radial direction (21) and number of elements in the axial direction (8). The internal pressure (162 N/mm^2) and required overstrain were input. The discretization resulted in a structure with 4158 nodes, 3360 elements, 12474 degrees of freedom and a frontal width of 1458. The number of global stiffness matrix coefficients was therefore reduced by 98.6%. Only 1.4% of the potential computer memory requirements was to be utilized, leading to efficient solutions. This semiautomatic pre-processor program generated the Cartesian global nodal coordinates, the global connectivity matrix and nodal arrays of interest.

The processor generated the element destination matrix, the nodal destination vector and the frontal width. The displacement formulation was considered, due to the relative ease of writing the associated computer program codes. The eight-noded isoparametric element with eight Gauss points, shown in Fig. 2, was chosen because it results in simplified numerical integration procedures when generating the stiffness matrices and is very accurate, particularly for simple geometries. A serendipity family of element shape functions satisfying the Lagrangian interpolation function requirements were chosen, since they are easily generated. In the elastic-plastic analysis, the material was assumed to have an elastic, perfectly plastic stress-strain curve and to obey the von Mises yield criterion. The incremental theory of plasticity [22] using the plastic stress-strain constitutive matrix (equations 1 and 2) was

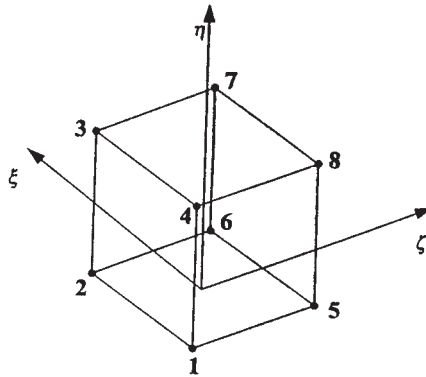


Fig. 2 Eight-noded brick element.

adopted. To obtain the displacements, Gauss point strains and stresses, the frontal solution technique [41–43] generated in this work was employed. Stress projection and nodal averaging followed by tensor transformation [44] were employed to obtain stress curves in the cylindrical coordinate system for the nodal arrays. Due to the accuracy of stress results, stress smoothing was found to be unnecessary.

The elastic analysis [45] was carried out using an internal pressure which would result only in elastic stresses. To proceed with elastic-plastic analysis [41], the maximum element effective stress, σ_{eff}^{max} , was obtained and all the element stresses, strains and displacements were raised by the factor of $\frac{Y_s}{\sigma_{eff}^{max}}$. Any element with an effective stress satisfying the condition $\sigma_{eff}^e \geq 0.95Y_s$ was considered to have yielded and its parameters were raised by the factor of $\frac{Y_s}{\sigma_{eff}^e}$. The element parameters were

stored. A small value of internal pressure equal to 0.1 N/mm^2 was applied and the analysis cycle repeated until the required overstrain. To obtain residual stresses, a negative internal pressure equal to the overstrain pressure was applied. To obtain the service stresses, an internal pressure less than the overstrain pressure was applied. To obtain material economy, the outer or bore radius of a cylinder having the same bore or outer radius and an incipient yield pressure equal to the overstrain pressure was determined. Various overstrains were considered. The overstrain resulting in the maximum material economy was considered to be the optimum.

In the elastic-plastic analysis, the Pradt–Reuss flow rule [22] was found adequate, though Nadai’s deformation theory [46] has also been shown to provide rapid iterative convergence. The matching of this later method with the frontal solution technique was found cumbersome to program. The load increment method [22] adopted in this work, though slower than other iterative schemes [47–49], is very suitable when there is a need to have many elements while the computer memory is limited (as in this work).

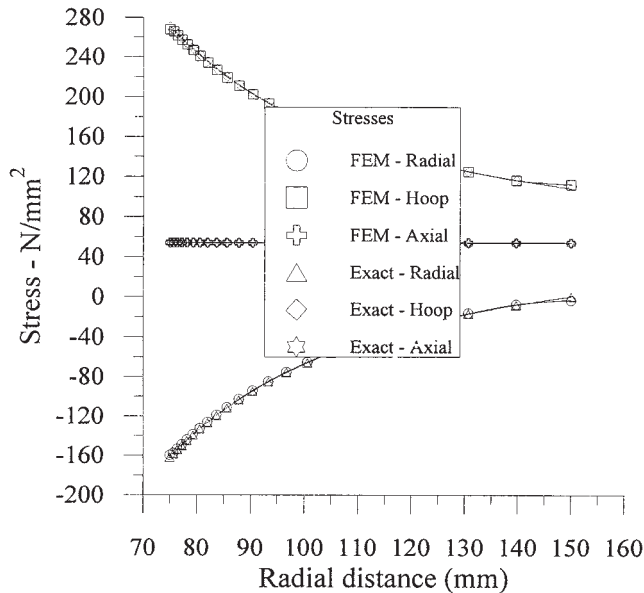


Fig. 3 *Elastic stresses.*

Results and discussion

Elastic response

The elastic stress distributions for both the analytical and FEM analysis are shown in Fig. 3. The curves are almost identical, confirming that in the elastic range the FEM analysis adopted is very accurate. At the cylinder bore, the percentage error in hoop stress is 1.109%. The stress curves reveal that there is a slight discrepancy in the FEM and analytical values of stress at the outside and inside surfaces of the cylinder for the hoop and radial stresses. This discrepancy is attributed to the weakness of conventional FEM in predicting surface stresses. This weakness has been addressed but not completely resolved by previous research [27–29]. In this work, the error in hoop stress at the bore is very small, whereas at the outside surface, which is not a critical point, the error did not justify further effort to improve the stress values. For points inside the material, the FEM results are very accurate. Higher geometric ratios gave more accurate results at the bore due to the finer mesh but reduced the accuracy on the outside. The geometric ratio of 1.15 was found to give the best results. The error phenomenon does not arise in the axial stress and this is attributed to lack of stress gradients in that direction. Fig. 4 shows the corresponding elastic displacements for FEM and analytical techniques and the results are almost identical.

Overstrain stresses

At 51% overstrain, the internal pressure applied was 327 N/mm² and the overstrain radius was 113 mm. Fig. 5 shows the effect of the 46 loading increments performed

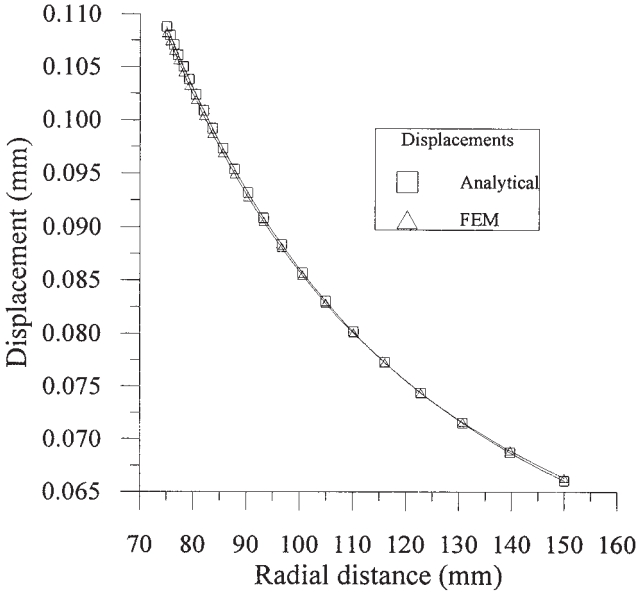


Fig. 4 Radial displacements.

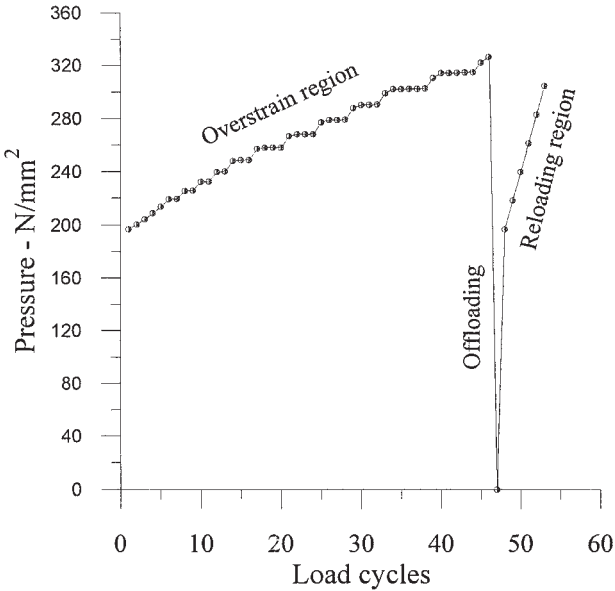


Fig. 5 Applied pressure vs. load cycles for 51% overstrain.

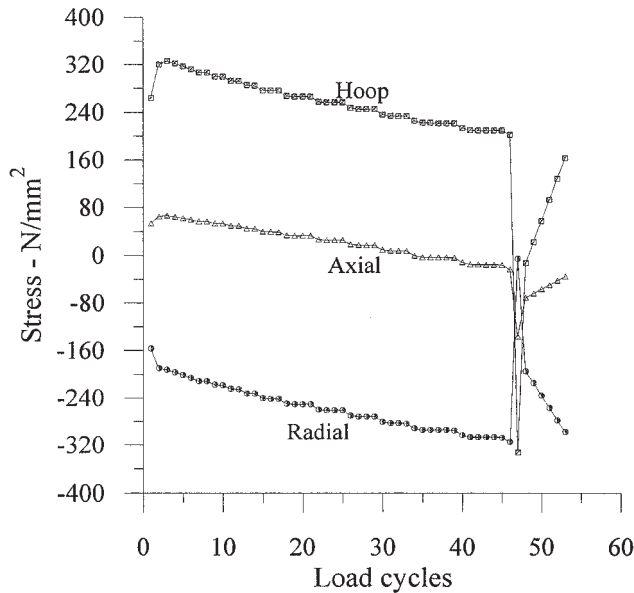


Fig. 6 Typical element overstrain stresses for 51% overstrain.

before the overstrain was attained. Six linear service increments were subsequently performed before re-yield. A staircase pattern is noticeable in the loading increments. This is because concentric elements will yield at around the same pressure. For less accurate work, the number of load increments could be reduced to the number of stair steps (25). This would greatly reduce the processing time and serves to demonstrate the expensive nature of the FEM. By using the modified yield condition method [22], only 3% of the potential processing time was used. This translates to a saving of 97% in time and expenses.

The variations of stresses in a typical element adjacent to the bore with the load increments for 51% overstrain are shown in Fig. 6. Beyond the yield point of the element, the hoop and radial stresses decrease as the internal pressure is increased. Upon offloading, negative residual stresses are evident. These stresses become positive upon further loading for the typical element. The radial stress increases numerically as the internal pressure is increased. The stress progression results for the typical element help in understanding the global response for elastic-plastic analysis.

Fig. 7 shows a comparison of the FEM and analytical solutions of the overstrain stresses for 51% overstrain. The results show that the FEM model adopted is accurate and reliable. The discrepancy at the outer surface is as discussed earlier. The overstrain axial stress distribution shows a 2% discrepancy over the elastic zone. This increases significantly as the plastic cylinder bore is approached but has no significant effect on the hoop and radial stresses. The intersection of the two curves is

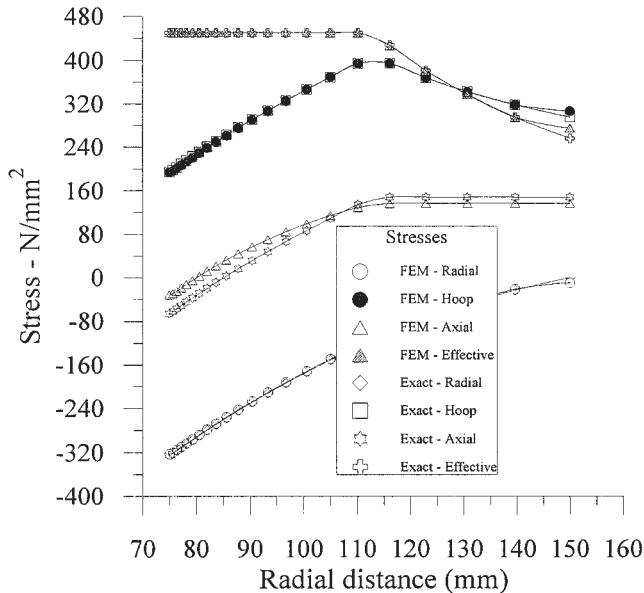


Fig. 7 Overstrain stresses for 51% overstrain.

not surprising, recalling that the FEM analysis gives an upper bound solution to the stiffness matrix and hence a lower bound to the stress solutions. The axial stress was found to be very sensitive to the discretization in the axial direction. A refined mesh in this direction was found to give more accurate results if the cylinder length was less than the wall thickness. However, practical analysis requires an infinite cylinder length and the results presented were a compromise between the two requirements. In most of the previous research work done in this area, the axial stress is seldom discussed, the reason being that it is a median stress and hence not the most critical. However, its influence on the effective stress should not be underestimated.

The nodal radial displacements for varying overstrains are shown in Fig. 8. The increase in displacements is most rapid at the bore. Whereas large overstrains may provide desirable stress distributions, they may also give rise to undesirable gross deformations during the overstraining process. Overstraining would also be detrimental in the presence of cracks at the bore. In this work, gross deformation was detected by a negative slope of the effective stress–strain curve as the analysis proceeded. Analysis of the 51% overstrain displacement curve shows element radial strains of 0.476% for the bore element and 0.068% for the outside radius element. This gives a strain ratio of 7, compared with a strain ratio of 5 in the elastic analysis.

Figs 9–12 show the overstrain stresses for varying degrees of overstrain. As the overstrain increases, the hoop and axial stresses at the bore increase in the negative sense and have a maximum value at the overstrain radius. For the cylinder geome-

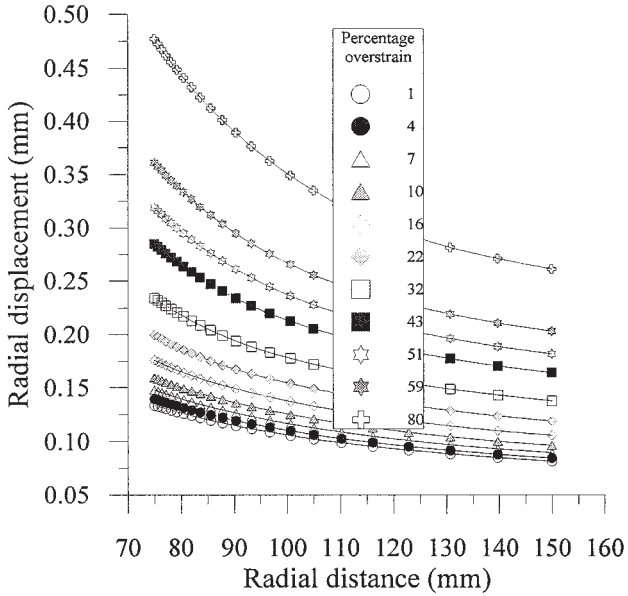


Fig. 8 Radial displacements for varying overstrains.

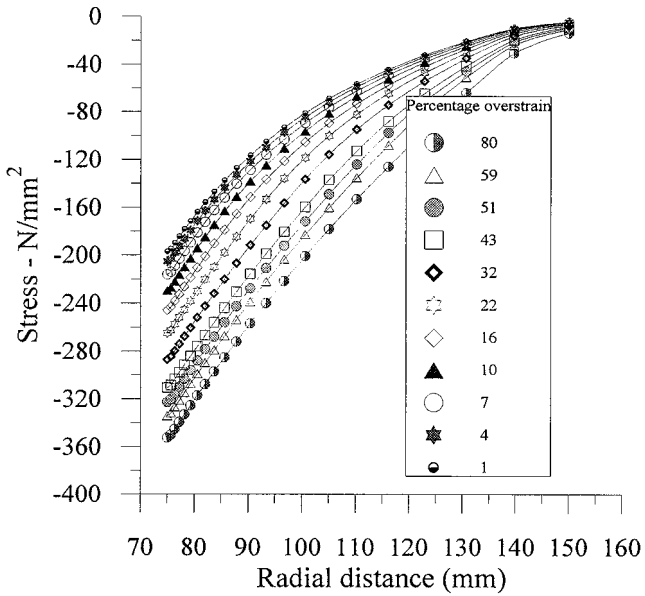


Fig. 9 Overstrain radial stresses for varying overstrains.

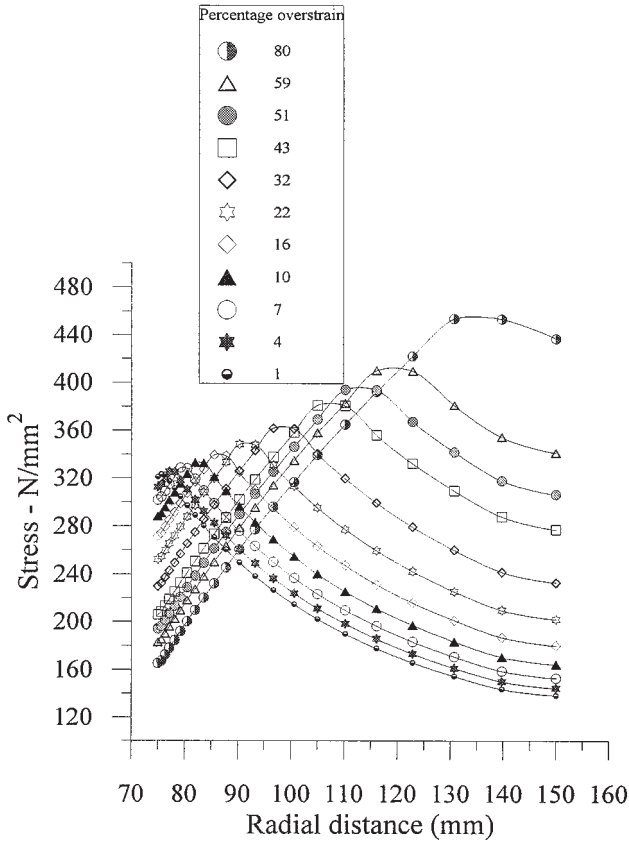


Fig. 10 Overstrain hoop stresses for varying overstrains.

try and material selected, it is then possible to make a fair estimate of the stress levels at intermediate overstrains.

Residual stresses

The residual stress results for 51% overstrain are shown in Fig. 13. The FEM results are very accurate for hoop and radial stresses. It is clear that the residual stress distribution is favourable, particularly with regard to the hoop stress, which is negative at the bore. The offloading was envisaged as a reversed linear loading by an amount equal to the last overstrain pressure of 327 N/mm². Some authors [22,50] describe the unloading path as being composed of a number of steps, while in this work the unloading was done in one linear step. In practice, the offloading has to be done in a number of steps in order to avoid collapse, especially for high overstrains.

The effective residual stresses for varying overstrains are shown in Fig. 14. Reverse yielding does not occur and, for each overstrain, the effective residual stress

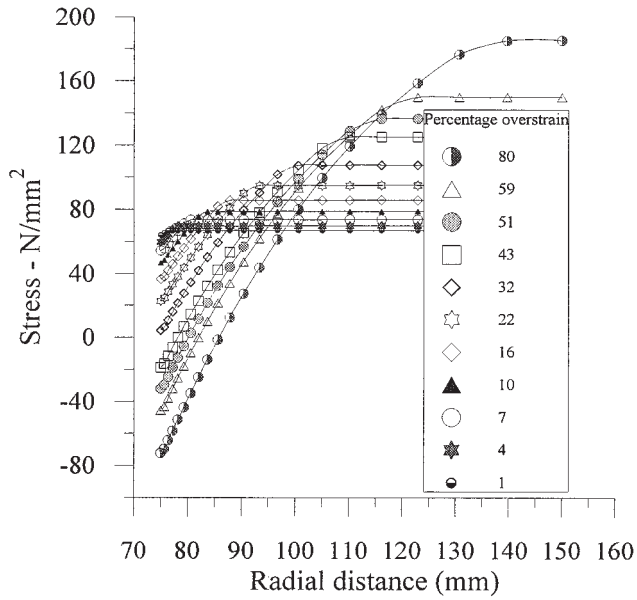


Fig. 11 Overstrain axial stress for varying overstrains.

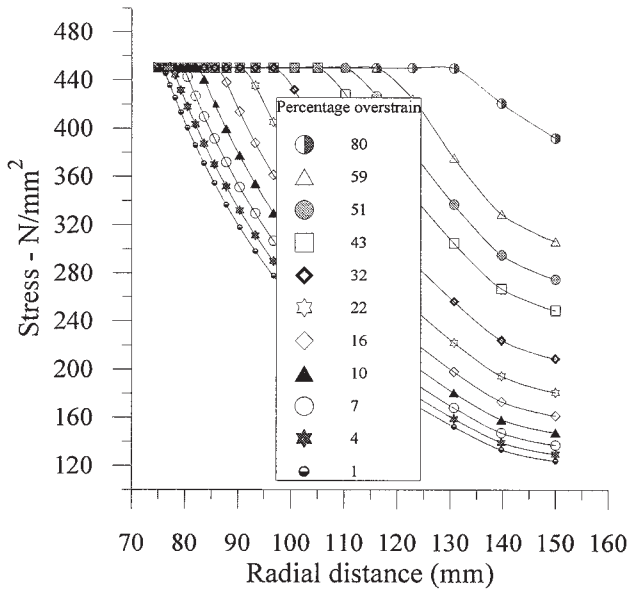


Fig. 12 Overstrain effective stresses for varying overstrains.

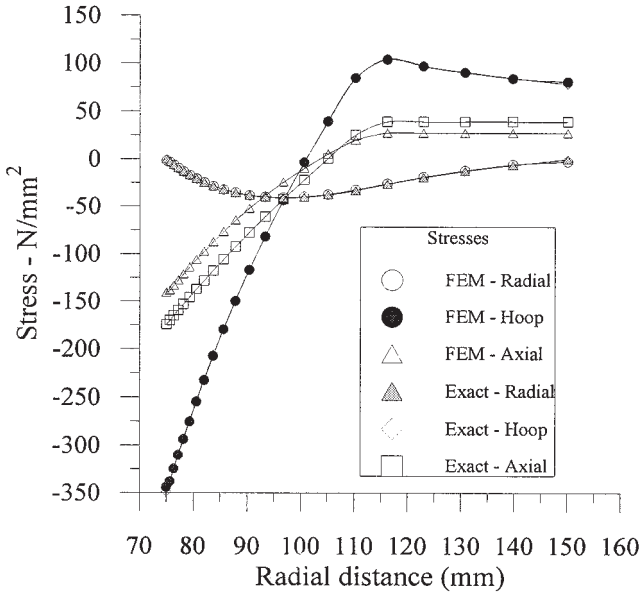


Fig. 13 Residual stresses for 51% overstrain.

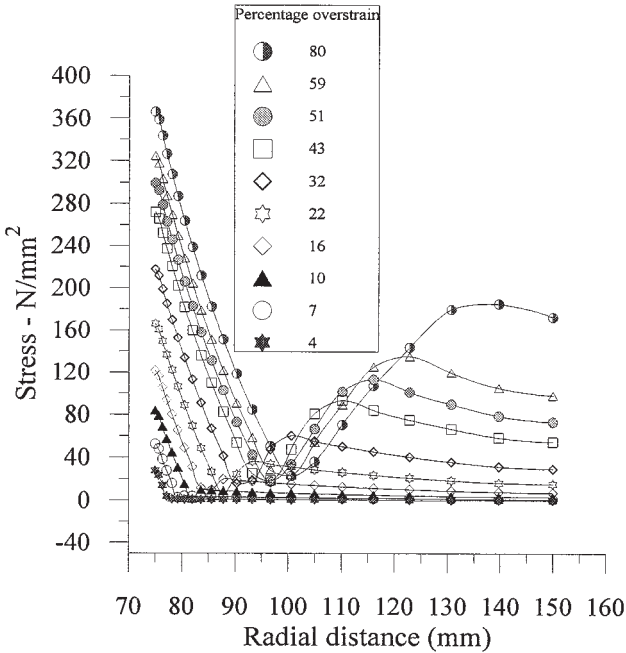


Fig. 14 Effective residual stresses for varying overstrains.

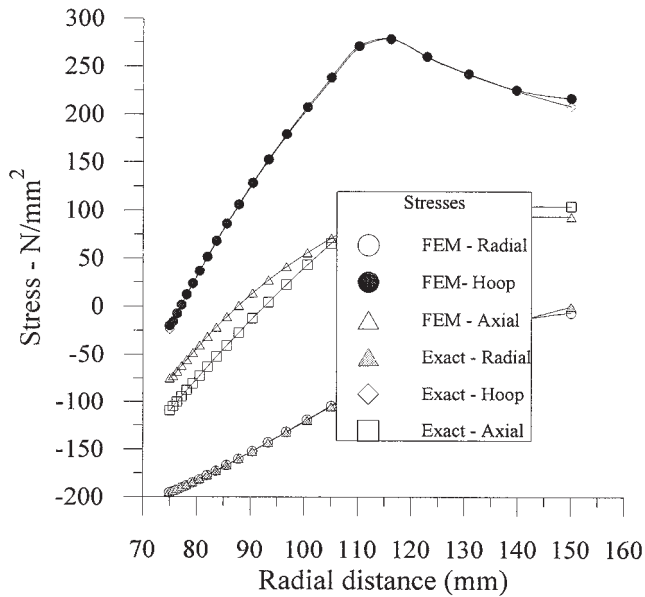


Fig. 15 Service stresses for 51% overstrain and a service pressure of 197 N/mm^2 .

curves have a minimum, but not at the respective overstrain radii. Overstraining should be so designed that reverse yielding due to residual stresses is avoided.

Service stresses

Fig. 15 shows the distribution of the service stresses with the applied pressure being equal to 197 N/mm^2 . The stresses at the bore are all negative and the maximum hoop stress occurs at the overstrain radius. Indeed, this is the major advantage of autofrettage. Below certain service pressures, it is then possible to have the bore permanently under compressive stresses. Should any crack have occurred at the bore, then it is always closed in service and its chances of propagation are greatly minimized. The maximum hoop stress of 275 N/mm^2 occurs at the overstrain radius. This is comparable to the maximum hoop stress of 275 N/mm^2 at the bore, for elastic analysis at a pressure of 162 N/mm^2 . As the service pressure is increased, the hoop stress at the bore is bound to increase to positive levels. This would lead to stress reversals, with the possibility of incremental collapse or low cycle fatigue. Despite the low hoop stress at the bore, it is therefore a critical point of the cylinder. If the service stresses are kept below zero, this possibility does not arise and the critical point remains at the elastic-plastic interface.

Fig. 16 shows the variations of effective service stresses at different levels of service internal pressures. It is seen that for any overstrain level, no re-yielding of the cylinder can occur until the full overstrain pressure is attained. It is also notable that the maximum effective stress occurs at the overstrain radius and failure is there-

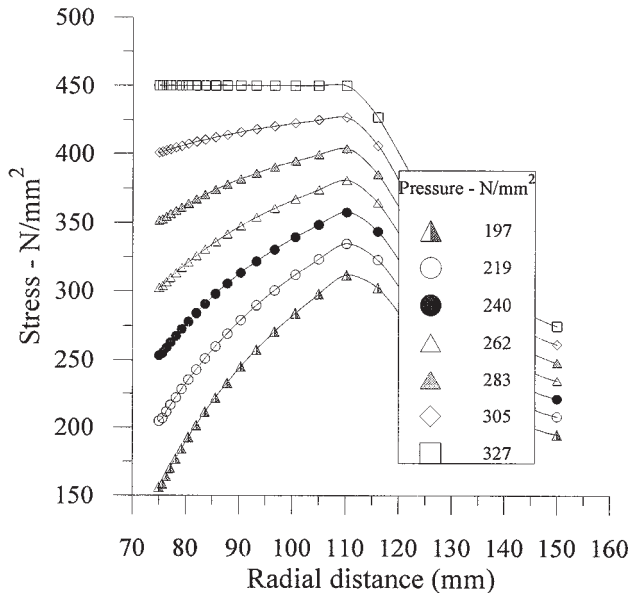


Fig. 16 Service effective stresses for 51% overstrain for varying service pressures.

fore likely to initiate at the overstrain radius. From a practical point of view, a crack starting at the inside, due to inclusions or other defects, is more difficult to detect and could require careful use of non-destructive testing techniques.

Economics of Autofrettage

Fig. 17 shows the re-yield pressure for various overstrains. As the overstrain is increased, the re-yield pressure increases. This means that, on re-loading, the cylinder can take up more pressure, before any new signs of material flow, than would be the case for the cylinder which has not been autofrettaged. For higher values of overstrain, the gain in re-yield pressure is less per unit overstrain increment. There are two ways of evaluating the material economy and hence the optimum overstrain. One approach is to consider a fixed bore radius and evaluate the outer surface radius that would experience incipient yielding at an internal pressure given by the re-yield pressure for the given overstrain. The other approach is to have a fixed outer radius of the cylinder and seek a bore radius that would lead to incipient yielding at the value of the re-yield pressure for the given overstrain. The results from these two approaches are shown in Fig. 18. The savings from the first method are clearly more than those obtained by considering the second method.

The percentage savings increase linearly as the limit of the internal pressure of 260 N/mm^2 is approached. For the cylinder to carry any pressure beyond this point, the yield stress needs to be increased, no matter what value of outside radius is used. Therefore, any discussion of the saving in material must be confined to the case

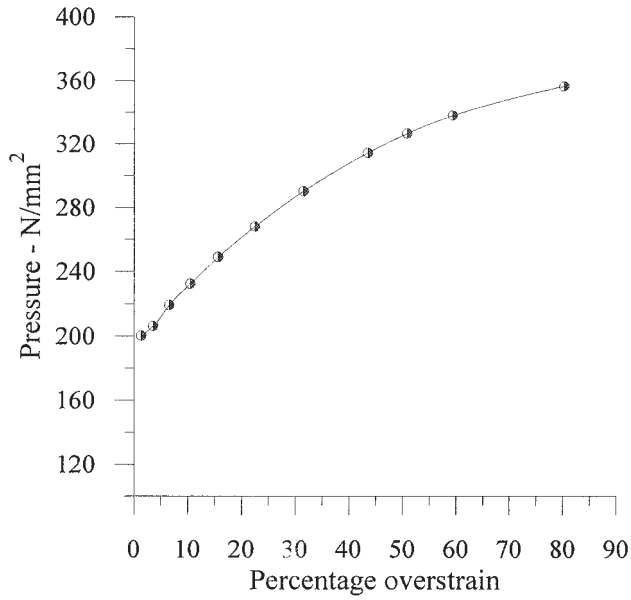


Fig. 17 Re-yield pressure for varying overstrain.

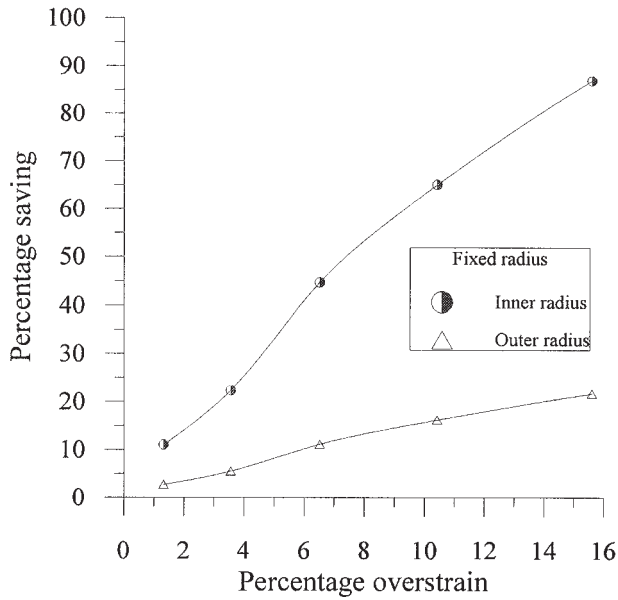


Fig. 18 Percentage material saving vs. overstrain for fixed radius.

where the internal pressure, P , is less than $Y_s/\sqrt{3}$. For the cylinder under consideration, the optimum overstrain is 16%. This gives an overstrain radius of $(R_i/R_o)^{0.48}$, which is 20% lower than the value obtained through other methods [33]. For the fixed bore radius, a much larger outside radius would be required. This would be a problem where dimensional, weight and cost limitations must be observed.

Conclusions and recommendations

The stresses and displacements obtained through a FEM analysis have been shown to be equal to those obtained through the analytical procedure. The FEM program developed in this work is therefore acceptable and may be reliably used in the analysis of more complex geometries and load conditions. The frontal solution procedure employed in this work allowed fine discretization and is suitable where there are limited computing facilities, as has been demonstrated. While the load increment method gives accurate results, it is very expensive. Autofrettage results in more favourably distributed stresses with negative hoop stresses at the bore. Stress reversals can be avoided by keeping the service stresses negative in overstrained cylinders. For cylinders having a thickness ratio of 2, the optimum overstrain is 16%.

The effect of large strains occurring during high overstrains, particularly at the bore, on the strain displacement matrix was not accounted for and needs to be investigated. The strain hardening behaviour of real materials needs to be accounted for in future research.

References

- [1] H. Ford, E. H. Watson and B. Crossland, 'Thought on a code of practice for forged high pressure vessels of monobloc design', *Transactions of ASME*, **103** (February 1981).
- [2] L. M. Masu and G. Craggs, 'Fatigue strength of thick walled cylinders containing cross bores with blending features', *Journal of Mech. Eng. Sci.*, **206** (1992), 299–309.
- [3] C. A. Zafec, 'Boiler embrittlement', *Transactions of ASME*, **66**(2) (1942), 81–126.
- [4] F. H. Daniels, 'An interesting boiler explosion', *Transactions of ASME*, **15** (1892), 118–146.
- [5] S. H. Bush, 'Statistics of pressure vessel and piping failures', *Journal of Pressure Vessel Technology*, **110** (1988), 225–233.
- [6] D. A. Lihou, 'Failures of liquefied gas storage vessels', *Journal of Process Mechanical Engineering*, **205** (1991), 27–31.
- [7] L. M. Davies, *et al.*, 'Second Marshall Study Group on PWR pressure vessel integrity', *Journal of Pressure Vessel Technology*, **105** (1983), 53–57.
- [8] M. T. Jacob, 'New rules for construction of section III, class I components for elevated temperature service', *Journal of Pressure Vessel Technology* (August 1976), 214–222.
- [9] BS 5500, 'Unfired Fission Welded Pressure Vessels, Section 3', 1991.
- [10] M. D. Bernstein, 'Design criteria for boilers and pressure vessels in the U.S.A.', *Journal of Pressure Vessel Technology* (November 1988), 430–443.
- [11] J. H. Faupel, 'Yield and bursting characteristics of heavy-wall cylinders', *Transactions of ASME* (1956), 1031–1064.
- [12] W. R. D. Manning, 'Bursting pressure as the basis for cylinder design', *Journal of Pressure Vessel Technology*, **100** (1978), 374–381.
- [13] B. Crossland, *et al.*, 'The strength of thick-walled cylinders', *Journal of Engineering for Industry* (May 1959), 95–114.

- [14] R. T. Stewart, 'Strength of steel tubes, pipes and cylinders under internal pressure', *Transactions of ASME, Cleveland* (1912), 297–318.
- [15] W. R. Burrows, 'A wall thickness formula for high-pressure, high-temperature piping', *Transactions of ASME* (April 1954), 427–444.
- [16] J. Marin and T. L. Weng, 'Strength of thick-walled cylindrical pressure vessels', *Journal of Engineering for Industry* (November 1963), 405–416.
- [17] C. Hwang, 'Incremental stress-strain law applied to work hardening plastic materials', *Journal of Applied Mechanics* (December 1959), 594–598.
- [18] D. C. Drucker, 'Relation of experiments to mathematical theories of plasticity', *Journal of Applied Mechanics* (December 1949), 349–357.
- [19] H. F. Bohnenblust and P. Duwez, 'Some properties of a mechanical model of plasticity', *Journal of Applied Mechanics* (September 1948), 222–225.
- [20] W. H. Warner and G. H. Handelman, 'A modified incremental strain law for work-hardening materials', *Quart. Journ. Mech. Applied Math.*, **9**(3) (1956), 279–293.
- [21] P. V. Marcal, 'A stiffness method for elastic plastic problems', *International Journal of Mechanical Science*, **7** (1965), 220–238.
- [22] Y. Yamada, et al., 'Plastic stress strain matrix and its application for the solution of elastic plastic problems by the finite element method', *International Journal of Mechanical Science*, **10** (1968), 343–354.
- [23] Y. Yamada and M. Koide, 'Analysis of bore expanding test by the incremental theory of plasticity', *International Journal of Mechanical Science*, **10** (1968), 1–14.
- [24] I. Pillinger, et al., 'Use of mean normal technique for efficient and numerically stable large strain elastic plastic finite element solutions', *International Journal of Mechanical Science*, **28**(1) (1986), 23–29.
- [25] D. R. G. Owen and E. M. Salonen, 'Three dimensional elastic plastic finite element analysis', *Int. J. Num. Meth. Engng.*, **9** (1975), 209–218.
- [26] S. Y. Cheng, et al., 'An integrated load increment method for finite elasto-plastic stress analysis', *Int. J. Num. Meth. Engng.*, **15** (1980), 833–842.
- [27] T. H. Richards and M. J. Daniels, 'Enhancing finite element boundary stress predictions for plane and axisymmetric situations', *Journal of Strain Analysis*, **21**(1) (1986), 33–44.
- [28] A. K. Soh, 'An improved method for determining free boundary stresses', *Journal of Strain Analysis*, **27**(2) (1992), 93–99.
- [29] T. H. Richards and M. J. Daniels, 'Enhancing finite element surface stress predictions: a semi-analytic technique for axisymmetric solids', *Journal of Strain Analysis*, **22**(3) (1987), 75–86.
- [30] P. C. T. Chen, 'The Bauschinger and hardening effect on residual stresses in an autofrettaged thick-walled cylinder', *Journal of Pressure Vessel Technology*, **108** (February 1986), 108–112.
- [31] D. W. A. Rees, 'Autofrettage theory and fatigue life of open-ended cylinders', *Journal of Strain Analysis*, **25**(2) (1990), 109–121.
- [32] R. J. Eggert, 'Design variation simulation of thick-walled cylinders', *Journal of Mechanical Design*, **117** (June 1995), 221–228.
- [33] S. M. Jorgensen, 'Overstrain and bursting strength of thick-walled cylinders', *Transactions of ASME*, **80**(3) (April 1958), 561–570.
- [34] M. Perl and R. Arone, 'An axisymmetric stress release method for measuring the autofrettage level in thick-walled cylinders – Part I: Basic concept and numerical simulation', *Journal of Pressure Vessel Technology*, **116** (November 1994), 384–388.
- [35] M. Perl and R. Arone, 'An axisymmetric stress release method for measuring the autofrettage level in thick-walled cylinders – Part II: Experimental validation', *Journal of Pressure Vessel Technology*, **116** (November 1994), 389–395.
- [36] R. Seshadri, 'Residual stress estimation and shakedown evaluation using GLOSS analysis', *Journal of Pressure Vessel Technology*, **116** (August 1994), 290–294.
- [37] H. Zhou and M. Rao, 'On the error analysis of residual stress measurements by the hole-drilling method', *Journal of Strain Analysis*, **28**(4) (1993), 273–276.
- [38] H. L. Stark, et al., 'A destructive procedure to determine the residual stresses in thick-walled cylindrical pressure vessels', *Journal of Strain Analysis*, **29**(1) (1994), 57–63.

- [39] M. A. Hussain, *et al.*, 'Simulation of partial autofrettage by thermal loads', *Journal of Pressure Vessel Technology*, **102** (August 1980), 314–318.
- [40] G. J. Mraz and E. G. Nisbett, 'Design, manufacture and safety aspects of forged vessels for high pressure service', *Journal of Pressure Vessel Technology*, **102** (1980), 99–106.
- [41] B. M. Irons, 'A frontal solution program', *Int. J. Num. Meth. Engng*, **2** (1970), 5–32.
- [42] E. Thompson and Y. Shimazaki, 'A frontal procedure using skyline storage', *Int. J. Num. Meth. Engng*, **15** (1980), 889–910.
- [43] S. F. Abbas, 'Some novel applications of the frontal concept', *Int. J. Num. Meth. Engng*, **15** (1980), 519–536.
- [44] E. Hinton and J. S. Campbell, 'Local and global smoothing of discontinuous finite element function using a least square method', *Int. J. Num. Meth. Eng.*, **8** (1974), 461–480.
- [45] J. M. Kihui and S. M. Mutuli, 'Time and space management in structural analysis problems', *International Journal of Mechanical Engineering Education*, **26**(4) (1998), 273–292.
- [46] H. O. Kim, 'A finite element formulation based on nadai's deformation theory for elasto-plastic analysis', *Int. J. Num. Meth. Engng*, **17** (1981), 1861–1876.
- [47] G. Powell and J. Simons, 'Improved iteration strategy for nonlinear structures', *Int. J. Num. Meth. Engng*, **17** (1981), 1455–1467.
- [48] E. F. Boyle and A. Jennings, 'Accelerating the convergence of elastic-plastic stress analysis', *Int. J. Num. Meth. Engng*, **7**(3) (1973), 232–235.
- [49] O. C. Zienkiewicz, *et al.*, 'Elasto-plastic solutions of engineering problems 'initial stress', finite element approach', *Int. J. Num. Meth. Engng*, **1** (1969), 75–100.
- [50] G. C. Nayak, 'Elasto plastic stress analysis: a generalization for various constitutive relations including strain softening', *Int. J. Num. Meth. Engng*, **5** (1972), 123.